RSC Advances

PAPER

View Article Online
View Journal | View Issue

Cite this: *RSC Adv.*, 2019, **9**, 41616

Preparation of a highly crosslinked biosafe dental nanocomposite resin with a tetrafunctional methacrylate quaternary ammonium salt monomer†

Weiguo Wang, ‡[a] Fan Wu,‡[a] Guoqing Zhang,[a] Sailing Zhu,[a] Jinghao Ban[b] and Limin Wang*[a]

The design of antimicrobial dental nanocomposite resin to prevent secondary dental caries and minimize biosafety problems is an important endeavor with both fundamental and practical implications. In the present work, a novel tetrafunctional methacrylate-based polymerizable quaternary ammonium monomer (TMQA) was synthesized with the aim of using it as an immobilized antibacterial agent in methacrylate dental composites, and its structure was characterized. The antibacterial action of TMQA and polymerized resin specimens against suspected cariogenic bacteria *Streptococcus mutans* were evaluated. Furthermore, the double bond conversion, contact angle, water sorption, solubility, heterogeneity, and crosslink density of the experimental resins with different concentrations of TMQA were investigated. CCK-8 and real-time cell analyses were used to evaluate the cytotoxicity of the experimental resins. The results showed that TMQA was successfully synthesized and had strong antibacterial properties against *Streptococcus mutans*. The experimental resins with different concentrations of TMQA had a similar degree of conversion and contact angle to the neat resin. With the addition of 4% TMQA to the resins, water absorption and solubility were reduced while their heterogeneity and crosslink density increased. The cell viability of each experimental group was similar to that of the neat resin group and was higher than that of the commercial adhesive single bond 2 group. Therefore, TMQA can be used to impart antibacterial properties to resins and increase the crosslink density of dental resin composites.

Received 5th November 2019
Accepted 10th December 2019

DOI: 10.1039/c9ra09173d

rsc.li/rsc-advances

1. Introduction

Dental caries is one of the most prevalent bacteria-related infectious diseases of the mouth.[1] During the development of dental caries, acidogenic and aciduric bacteria such as *Streptococcus mutans* accumulate on teeth and dental fillings and can cause enamel and dentin demineralization through acid generation.[2] Following demineralization, degradation of the demineralized collagen matrix is induced by salivary proteases or endogenous peptidases such as matrix metalloproteinases (MMPs) and cysteine cathepsins.[3] Dental caries is not a self-healing disease and must be filled with suitable materials. Many materials such as amalgam, glass ionomer, and dental composite resin have been used for restoring decayed teeth.[4] Among these, dental composite resins with adhesive systems based on methacrylate monomers have gradually replaced other materials owing to their better aesthetics and improved properties.

However, the clinical life of dental resin is significantly shorter than amalgam,[5] mainly because of secondary caries at the tooth–resin interface. According to a previous study, bacteria are more likely to adhere to dental nanocomposite resins than porcelain, amalgam, and glass ionomer.[6,7] In addition, the polymerization shrinkage stress of dental nanocomposite resins produced in a polymerization reaction leads to gaps between the tooth and the resin. Bacteria adhering to these gaps are difficult to clean and cause secondary caries at the tooth–resin interface.[8] Therefore, resins with strong and long-lasting antibacterial properties are highly desirable.[9]

Currently, there are three main ways to manufacture biological materials with antibacterial properties: adding the organic antibacterial agent directly, packaging the inorganic antibacterial agent, and using a polymeric antibacterial agent[10] The effect of an inorganic or organic antibacterial agent on

[a]*Department of Stomatology, No. 903 Hospital of PLA, Lingyin Road 14, Hangzhou, 310000, People's Republic of China. E-mail: wlm117@126.com; Fax: + 86 571 8734 0983; Tel: + 86 571 8734 0983*

[b]*School of Stomatology, Fourth Military Medical University, Xi'an, People's Republic of China*

† Electronic supplementary information (ESI) available. See DOI: 10.1039/c9ra09173d

‡ These two authors contributed equally to this work as co-first authors.

antibacterial modification is dependent on the dissolution of antibacterial components, so it has a short-term antibacterial effect, reduces the mechanical properties, affects the color stability, decomposes toxic substances, and other disadvantages.[11–15] Polymeric antimicrobial agents are permanently copolymerized with resin materials by forming covalent bonds with polymer networks. This stable nonleaching antimicrobial material provides long-term protection by killing microorganisms that come into contact with the resin surface, and does not sacrifice the original mechanical properties and polymerization behavior of the resin material.[16–18]

Compared with other methods, the addition of quaternary ammonium salt (QAS) monomer to polymers by using antimicrobial monomers is one of the most promising strategies for the preparation of antimicrobial biomaterials. The QAS monomer is a polymerizable antimicrobial agent. Before polymerization, it behaves like other traditional antibacterial agents that can freely play an antibacterial role. When the QAS monomer is polymerized into the resin matrix, the resin has antibacterial effects through the N^+ ions and long lengths of alkyl chains on its surface.[19] The antibacterial mechanism of QAS monomers is the same as that of general nitrogen-containing cationic antibacterial agents in which the negatively charged bacterial cell wall attracts the positive quaternary amine charges on N^+ ions.[20] The QAS monomer can adsorb to the bacteria and insert a lipophilic side-chain tail into the bacterial cell membrane. This disturbs the electrical balance of the cell membranes and leads to the destruction of the integrity of cell membranes, leakage of cell contents, and the death of the bacterial cell. In addition, a QAS monomer can destroy bacterial proteins and enzymes.[21] Studies have shown that while the surface of the material has low N^+ ion content, it can inhibit bacterial growth and exhibit bacteriostatic action. When the N^+ ion content is high, the bacterial cell membrane can be quickly destroyed, and the bacteria can be killed.[22] When the addition amount of the QAS monomer increases, the density of the N^+ ions on the surface of the photocurable composite resin material also increases; thus, materials with excellent antibacterial performance can be obtained. However, the capability of a resin polymer network to copolymerize with QAS monomers is limited.

At present, the QAS monomer generally contains one or two methacrylate groups. The earliest developed monomethacrylate QAS monomer (*i.e.*, QAS with one methacrylate group) was dangled in the polymer network,[23–25] while the later difunctional methacrylate QAS monomer (*i.e.*, QAS with two methacrylate groups) was formed into a chain structure and grafted into the resin matrix.[26–29] Regardless of the number of methacrylate groups, the major problem with recent QAS monomers is the precipitation caused by the low crosslinking density, which results in a decrease in the physical and biosafety properties of the copolymer.[10,30–32] To solve these problems, QAS monomers with more than two methacrylate groups are desirable. Jaymand *et al.* suggested that multifunctional and dendritic monomers can be used to improve the crosslinking degree and performance of the resin.[33–35] Monomers with multifunctional methacrylate groups provide a very high number of functional groups in a compact space that has high reactivity and can become a crosslinking center of the polymer.[36]

There have been few studies on QAS monomers with multifunctional methacrylate groups. The present research work involves the formulation and characterization of a novel QAS monomer containing tetrafunctional methacrylate groups with long lengths of alkyl chains. A tetrafunctional methacrylate quaternary ammonium (TMQA) monomer was synthesized under controlled conditions through a three-step chemical procedure. The hypothesis in this study is that the incorporation of TMQA in experimental resins can improve the crosslinking degree and display acceptable cytotoxicity.

2. Experimental

2.1 Synthesis of intermediate-product

In a 250 mL three-necked round-bottom flask, *N*-methylethanolamine (10 mL, 87.08 mmol) was dissolved in 90 mL of acetonitrile solution. Then, 1-bromododecane (21 mL, 87.2 mmol) was added to the reaction mixture using a dropping funnel. The reaction mixture was stirred and heated to reflux under nitrogen protection for about 36 h. At the end of this period, the reaction was completed with the color of the solution changing from colorless to light yellow. Then, the solution was placed in a refrigerator until a large amount of white solid precipitate was formed. This was filtered and washed with acetonitrile to obtain 26.15 g of white product *N*,*N*-bis(2-hydroxyethyl)-*N*-methyldodecan-1-aminium bromide (HQA). ^{1}H NMR (400 MHz, $CDCl_3$) δ: 0.82–0.89 (3H, $-CH_3$), 1.23–1.38 (18H, $-CH_2-$), 1.67–1.83 (2H), 3.31–3.39 (3H, N^+-CH_3), 3.44–3.53 (2H, N^+-CH_2-), 3.67 to 3.83 (4H, N^+-CH_2-), 4.07 to 4.19 (4H, $O-CH_2-$), 4.62 to 4.79 (2H, –OH).

2.2 Synthesis of TMQA

In a 250 mL three-necked round-bottom flask, HDI (23.78 g, 141.5 mmol) was stirred to dissolve in 30 mL of acetone at room temperature. In a separate container, HQA (26.15 g, 70.8 mmol) was dissolved in 50 mL of acetone, then added to the reaction mixture dropwise using a dropping funnel and reacted at 25 °C for 5 h under nitrogen protection. Next, 2-hydroxypropylene glycol dimethacrylate (33.0 g, 145 mmol), 0.25 g of hydroquinone, and an appropriate amount of acetone were added to the reaction mixture, and the reaction was carried out at 55 °C for 14 h. Then, the solvent was evaporated using a rotary evaporator. The product was washed with diethyl ether and centrifuged to remove hydroquinone and unreacted 2-hydroxypropylene glycol dimethacrylate. FT-IR (cm^{-1}): ν_{N-H} = 3326 (s), ν_{C-H} = 2931 (s), $\nu_{C=O}$ = 1709 (s), $\nu_{C=C}$ = 1637 (m), δ_{C-H} = 1455 (s), ν_{C-N} = 1250 (s), ν_{C-O} = 1154 (s). ^{1}H NMR (400 MHz, DMSO-d_6) δ: 0.81–0.9 (3H, $-CH_3$), 1.13–1.58 (34H, $-CH_2-$), 1.65–1.81 (2H, $-CH_2-$), 1.83–1.95 (12H, $-CH_3$), 2.81–3.21 (8H, $N-CH_2-$), 3.21–3.41 (3H, N^+-CH_3), 3.41–3.56 (2H, N^+-CH_2-), 3.56–3.82 (2H, O–CH–), 3.82–4.19 (4H, N^+-CH_2-), 4.19–4.33 (8H, $O-CH_2-$), 4.41–4.61 (4H, $O-CH_2$), 5.59–5.62 (4H, Allyl-H), 6.05–6.21 (4H, Allyl-H), 6.65–6.88 (4H NH). ^{13}C NMR (150 MHz, DMSO-d_6): δ(ppm): 169.4, 158.3, 138.8, 128.8, 75.5, 69.2, 68.4, 63.6, 60.2,

52.0, 43.3, 34.4, 32.4, 32.1, 32.0, 31.8, 31.7, 29.1, 28.9, 25.2, 20.93, 20.89, 20.83, 16.9 ppm. MS (MALDI-TOF): calcd for $C_{55}H_{94}N_5O_{16}$ $[M + H]^+$ 1080.669, found 1080.665. Elemental analysis calcd (%) for $C_{55}H_{94}$ Br N_5O_{16}: C, 56.89; H, 8.16; N, 6.03. Found: C, 56.77; H, 8.20; N, 5.91.

2.3 Characterization

The FTIR spectra of synthesized materials were recorded on a FTIR spectrometer (Nicolet IS50, Thermo Scientific Co., USA) in the wavenumber range from 4000 to 400 cm^{-1} with a resolution of 4 cm^{-1}.

^1H spectra were recorded using a Bruker Avance 400 spectrometer (400 MHz, Bruker, Germany). The sample for ^1H NMR spectroscopy was prepared by dissolving a sample of about 10 mg in 1 mL of deuterated dimethyl sulfoxide (DMSO-d_6). ^{13}C NMR spectra were recorded using an Agilent 600 MHz DD2 spectrometer (600 MHz, Agilent, USA). The sample for ^{13}C NMR spectroscopy was prepared by dissolving a sample of about 50 mg in 1 mL of deuterated dimethyl sulfoxide (DMSO-d_6). Exact mass was obtained through Matrix Assisted Laser Desorption Ionization Time of Flight mass spectrometry (MALDI-TOF MS, Bruker Daltonics, USA). Elemental analyses. Elemental analyses (C, H, and N) were performed using a Vario Micro element analyzer (Elenemtar Analysensysteme GmbH, Germany).

2.4 Preparation of resin formulations

Bisphenol A glycerolatedimethacrylate (bis-GMA), tri(ethyleneglycol) dimethacrylate (TEGDMA), camphorquinone (CQ), and ethyl 4-dimethylamino-benzoate (EDMAB) were purchased from Sigma-Aldrich (St. Louis, MO, USA). First, the resin was prepared at bis-GMA : TEGDMA weight ratios of 50 : 50. Then, TMQA and MAE-DB was added to the resin in specified proportions. Finally, 0.5% CQ and 1% EDMAB were added to the comonomer blends as the photo initiator and accelerator, respectively. The specific code and addition ratio are listed in Table 1. All resin comonomer blends were homogenized and stored in the dark before use.

2.5 Antibacterial activity test

2.5.1 Antibacterial properties of TMQA. *Streptococcus mutans* (UA 159) was inoculated in sterile brain heart infusion (BHI) broth (Difco, Becton-Dickinson and Co., Sparks, MD, USA) and cultured overnight at 37 °C in an anaerobic incubator. The resulting bacterial suspension was diluted to a concentration of 1×10^6 colony forming units (CFU) per mL for further use. The minimum inhibitory concentration (MIC) and minimum bactericidal concentration (MBC) values of TMQA were determined in this test, where 2-methacryloxylethyl dodecyl methyl ammonium bromide (MAE-DB) and chlorhexidine acetate were the positive control groups. The unpolymerized TMQA, MAE-DB, and chlorhexidine acetate were dissolved in BHI broth to produce an initial concentration of 1 mg mL^{-1}. From the starting solutions, serial twofold monomer dilutions were made into 1 mL volumes of culture solution. Then, 100 μL of the microbial suspensions prepared in the previous step was added to each tube containing 1 mL of a series of antibacterial monomer dilution broths. After 24 h of anaerobic incubation, the tubes were read for turbidity. The MIC was defined as the endpoint where no turbidity could be detected with respect to the control groups. Then, 100 μL of the solutions in each well with concentrations higher than the MIC was taken out and plated on BHI plates. After 48 h of anaerobic culture, the bacteria colonies were recorded. The MBC value was defined as the lowest concentration of antibacterial monomers without bacterial growth on the plate. The tests were performed in triplicate.

2.5.2 Antibacterial properties of polymerized resin specimens. Experimental polymerized resin disks were fabricated using a cylindrical Teflon mold with an internal diameter of 10 mm and a height of 2 mm between two glass slides. The resin was polymerized for 60 s using a dental light source. The resin disks were then sterilized with ethylene oxide gas, followed by degassing for 48 h. *Streptococcus mutans* was inoculated in a sterile BHI broth and cultured overnight at 37 °C in an anaerobic incubator. The resulting bacterial suspension was diluted to a concentration of 1×10^6 colony forming units (CFUs) per mL for further use. The sterile specimens were placed in the wells of a 24-well plate with a 2 mL BHI broth. Then, 20 mL of a diluted *Streptococcus mutans* suspension was added to each well and incubated at 37 °C for 24 h under an anaerobic atmosphere to generate the biofilms. The disks coated with biofilms were then gently rinsed three times with sterile PBS to remove planktonic bacteria and the culture medium. In a new sterile 24-well plate, the specimens were soaked in 3% glutaraldehyde at 4 °C overnight, dehydrated in a graded series of ethanol solutions, and then dried in a critical-point drier. After a sputter coating of the samples with gold using an ion sputter (JFC-1100E, JEOL, Tokyo, Japan), all specimens were observed through a field emission SEM (FESEM; S-4800; Hitachi Ltd, Tokyo, Japan).

Specimens coated with a *Streptococcus mutans* biofilm were prepared as described above. The biofilm-coated disks were rinsed three times with sterile saline to remove any loose bacteria and then placed in a 24-well plate. Next, 1 mL of a Live/Dead Bac Light Bacterial Viability Kit L13152 (Molecular Probes, Invitrogen, Eugene, OR, USA) was added to each well to cover the sample, which was then incubated for 15 min at room temperature in the dark for fluorescent staining. Using this kit, live bacteria are stained using Syto 9, producing a green

Table 1 Compositions of dental resin systems

	Composition of resin (wt%)					
Resin	BIS-GMA	TEGDMA	TMQA	MAE-DB	CQ	EDMAB
TM0	49.25	49.25	0	0	0.5	1
TM1	48.75	48.75	1	0	0.5	1
TM4	47.25	47.25	4	0	0.5	1
TM7	45.75	45.75	7	0	0.5	1
TM10	44.25	44.25	10	0	0.5	1
DB4	47.25	47.25	0	4	0.5	1

fluorescence, and bacteria with compromised membranes are stained by propidium iodide, producing a red fluorescence.[37,38] The stained samples were washed with sterile saline and observed using a laser confocal microscope under dual-channel scan mode. Excitation with a 488 nm laser showed a green fluorescence emission of the live bacteria, and excitation with a 543 nm laser showed a red fluorescence emission of bacteria with damaged membrane.

2.6 Measurement of contact angle

Polymerized resin disks ($n = 5$) were fabricated using a cylindrical Teflon mold with an internal diameter of 10 mm and a height of 1 mm between two glass slides. The resin was polymerized for 60 s using a dental light source. The disks were polished with 1200 mesh sandpaper to smooth both sides. A video-based contact angle measuring device (Dataphysics Instruments, Filderstadt, Germany) was used to measure the contact angles of MilliQ water dispensed on the resin disk surface. A 2 μL drop of water was dropped on the surface of the sample to measure the contact angle. For each resin disk, the static contact angle obtained at 30 s was taken as the equilibrium contact angle.

2.7 Measurement of degree of conversion (DC)

The DC was measured using Fourier transform infrared spectroscopy (Nicolet IS50, Thermo Scientific Co., USA) at a resolution of 4 cm^{-1} and 32 scans in the range of 4000–400 cm^{-1}. Each sample was coated on a KBr plate and recorded on the FTIR spectrometer before curing. Then, the sample was covered with mylar film and photocured for 20 s. Next, the film was removed, and the sample was examined 5 min later. The DC was determined from the ratio of the absorbance intensities of the aliphatic C=C bonds (peak at 1637 cm^{-1}) against the internal reference aromatic C=C bonds (peak at 1607 cm^{-1}) before and after curing of the specimen. The degree of conversion was calculated as follows:

$$\mathrm{DC}(\%) = \left[1 - \frac{(1637\ \mathrm{cm^{-1}}/1607\ \mathrm{cm^{-1}})\text{peak area cured}}{(1637\ \mathrm{cm^{-1}}/1607\ \mathrm{cm^{-1}})\text{peak area uncured}}\right] \times 100$$

2.8 Measurement of water sorption, solubility, and diffusion coefficient

Dental resins were added to a cylindrical Teflon mold with an internal diameter of 15 mm and height of 1.0 mm, and then light-cured for 60 s with a dental light source. Five specimens of each sample were prepared. The specimens were placed in a desiccator at room temperature under normal pressure and weighed every 24 h until a constant mass (M_1) was obtained (*i.e.*, the variation was less than 0.001 g in any 24 h period). Then, the specimens were immersed in distilled water. At 1, 3, 6, 9, and 12 h on the first day and every 24 h thereafter, they were removed from the vials, washed in running water, blotted dry to remove excess water, weighed (M_t), and then returned to the water. The equilibrium mass (M_2) was obtained when there was no significant change in the mass. The specimens were then dried at 40 °C until their mass was constant, and the result was recorded as M_3. The water sorption (WS) and solubility (SL) were then calculated using the following formulas:

$$\mathrm{WS} = \frac{M_2 - M_3}{V} \times 100\%$$

$$\mathrm{SL} = \frac{M_1 - M_3}{V} \times 100\%$$

The diffusion coefficients of water (D) into the dental resins were determined by plotting the $\Delta M_t/\Delta M_2$ ratios as a function of the square root of time (where ΔM_t is the mass gain after time t, and ΔM_2 is the final mass gain). Since all plotted curves were linear when $\Delta M_t/\Delta M_2 \leq 0.5$ (Fig. 4), the diffusion coefficients of water in the resins could be calculated using Stefan's approximation:[39,40]

$$\frac{\Delta M_t}{\Delta M_2} = \frac{4}{L}\left(\frac{Dt}{\pi}\right)^{\frac{1}{2}},$$

where L is the thickness of the sample, and t is the storage time.

2.9 Dynamic mechanical analysis (DMA)

DMA tests were performed on a dynamic mechanical analyzer (DMA Q800, TA Instruments Co., USA) in three-point bending mode. Bar-shaped specimens (30 mm × 4 mm × 2 mm) were prepared in a Teflon mold. The measurement was conducted at a temperature range from 0 °C to 250 °C at a frequency of 1 Hz (approximate average chewing rate) and a heating rate of 5 °C min^{-1}. The storage modulus and tan δ were plotted against the temperature over this period. A typical storage modulus and tan δ curve of the experimental materials are shown in Fig. 6A. The temperature at the maximum in the tan δ curve was taken as the glass transition temperature (T_g). The width at the half-height of the tan δ curve (ΔT) reflects the heterogeneity of the polymer network. The crosslink density was calculated from the storage modulus in a rubbery plateau according to the rubber elasticity theory in the following equation:[41,42]

$$\upsilon = \frac{E'}{3\rho RT}$$

where υ is the crosslink density (mol kg^{-1}), E' is the storage modulus (MPa) at T_g + 30 °C, ρ is the density (g mL^{-1}), R is the gas constant (8.314472 J mol^{-1} K^{-1}), and T is the absolute temperature at T_g + 30 °C.

2.10 Cytotoxicity and viability experiments

The material cytotoxicity was evaluated *via* an extraction method. The commercial bond single bond 2 (SB group), which has been used clinically for a long time, was used as a standard control. Extracts were obtained from specimens incubated for 24 h at 37 °C in Dulbecco's modified Eagle medium (DMEM, GIBCO, USA) containing 10% fetal calf serum (FCS). The specimens (surface area of specimen/extraction volume was 1.25

cm^2 mL^{-1}) were sterilized by ultraviolet irradiation for 30 min on both sides, and then placed in a sterile centrifuge tube. The specimens were extracted in DMEM containing 10% FCS at 37 °C for 24 h, and were sterilized by filtration using a 0.22 μm filter. From the starting solutions, serial twofold extract dilutions were made into gradient concentrations of the culture solution. Then, 100 μL of the microbial suspensions prepared in the previous step was added to each tube containing 1 mL of a series of antibacterial monomer dilution broths.

L929 mouse fibroblast was purchased from the Shanghai Institutes for Biological Sciences (SIBS), Chinese Academy of Sciences (Shanghai, China), and was used to investigate the cytotoxicity of the materials. The cells were maintained in DMEM supplemented with 10% FCS, 100 units per mL of penicillin, and 100 μg mL^{-1} of streptomycin in a humidified incubator containing 5% CO_2 at 37 °C. Cells from passage numbers 4–6 were used for the experiments.

2.10.1 CCK-8 test and cell morphology. The cell line of the exponential growth phase was trypsinized to prepare a single-cell suspension of 2.5×10^4 cells per mL. The cell suspension was inoculated into a 96-well culture plate at 200 μL per well (5000 cells per well) and incubated for 24 h to allow for cell adhesion. The culture medium was then replaced by 200 μL of extract from each material except for the negative control group (NC group, culture medium without extract). Cells exposed to 200 μL of DMEM containing 10% FCS served as the control group. After incubations of 1, 3, and 5 days, the cell viability was assessed using Cell Counting Kit-8 (CCK-8 kit, APE BIO, USA) according to the manufacturer's instructions. For this process, 20 μL of CCK-8 dye solution was added to each well, and the cells were incubated for an additional 4 h.[43] Wells containing 200 μL of DMEM with 10% FCS and 20 μL of CCK-8 but without cells served as the blank control. The absorbance at 450 nm of the solution in each well was measured using a microplate reader (SpectraMax M5, Molecular Devices, Sunnyvale, CA, USA). The relative growth rate (RGR) of the cells was calculated using the following equation:

$$\mathrm{RGR} = \frac{\text{Mean absorbance value of experimental group}}{\text{Mean absorbance value of control}}$$

The images of each well containing the cells exposed to the extractions were visualized on a LAS V4.9 phase contrast trinocular microscope (Lecia, Germany) and were photographed.

2.10.2 Real-time cell analysis. The real-time cell viability was assessed and monitored using a real-time cell analyzer (RTCA, xCELLigence system, ACEA Biosciences, Germany). The instrument uses noninvasive electrical impedance monitoring to quantify the cell proliferation, morphology changes, and attachment quality in a label-free, real-time manner. RTCA was used according to the supplier's instructions. The background impedance of the E-plate was determined by adding 50 μL of the culture medium or the extract obtained in the previous step to each well and subtracted automatically by the RTCA software following the equation $\mathrm{CI} = (Z_i - Z_0)/15$, with Z_i as the impedance at any given time point and Z_0 as the background signal.[44] Subsequently, a 150 μL cell suspension containing 10^4 of L929 mouse fibroblast cells was seeded in each well of the E-plate 96 and allowed to settle at the bottom of the wells for 20 min before impedance measurement was begun in 15 min intervals.

2.11 Statistical analysis

All of the results except for those of the MIC and MBC were statistically analyzed and compared using one-way ANOVA and Tukey's test at a significance level of 0.05. The results for the MIC and MBC were statistically analyzed using a Kruskal–Wallis H test at a significance level of 0.05.

3. Results

3.1 Synthesis of TMQA

As shown in Fig. 1, TMQA was synthesized *via* a three-step route. First, intermediate compound HQA was prepared by reacting *N*-methyl diethanol amine with bromododecane through a Menschutkin reaction. Then, the HQA was reacted with HDI to form isocyanate terminated urethane precursors. Finally, TMQA was obtained by the reaction of isocyanate-terminated urethane precursors with 2-hydroxypropylene glycol dimethacrylate.

3.2 Characterization of TMQA

3.2.1 FTIR. The characteristic peak of the isocyanate group (2270 cm^{-1}) and the characteristic peak of the hydroxyl group (3290 cm^{-1}) were disappeared in the FTIR spectra, indicating that the isocyanate groups in the HDI have completely reacted with the hydroxyl groups in the HQA and 2-hydroxypropylene glycol dimethacrylate. The successful introduction of the carbamate group and the methacrylate group in the molecule indicates that the structure of the obtained product is consistent with the designed target product TMQA.

3.2.2 NMR. The ^{1}H NMR spectrum was used to confirm the chemical structure of the actual products, which is consistent with the designed structure. The chemical shifts at 1.13–1.58 ppm are attributed to 34 protons in the methylene group ($N^+CH_2CH_2(CH_2)_9CH_3$ and $NHCH_2(CH_2)_4CH_2NH$). Distinctive signal related to methyl and methylene groups appended to the quaternary ammonium were assigned at δ 3.21 to 4.19 ppm, which means the alkyl bromide has already reacted with *N*-methyl diethanol amine to form the quaternary ammonium structure. Absorption peaks around 1709 cm^{-1} and 1636 cm^{-1} in FT-IR spectra, chemical shifts around 6.05–6.21 ($CH_2{=}C(CH_3)$ *trans*), 5.59–5.62 ($CH_2{=}C(CH_3)$ *cis*) and 1.83–1.95 ($CH_2{=}C(CH_3)$) in the ^{1}H-NMR spectra reveal that there were methacrylate groups in the products. All these results demonstrate that the monomer TMQA has been successfully synthesized.

3.3 Antibacterial properties

The MIC/MBC values of the three materials determined for *Streptococcus mutans* are listed in Table 2. *Streptococcus mutans* is a suspected cariogenic bacterium. Although the data for TMQA are smaller than those for chlorhexidine acetate and MAE-DB monomer on some MIC/MBC values, its antibacterial

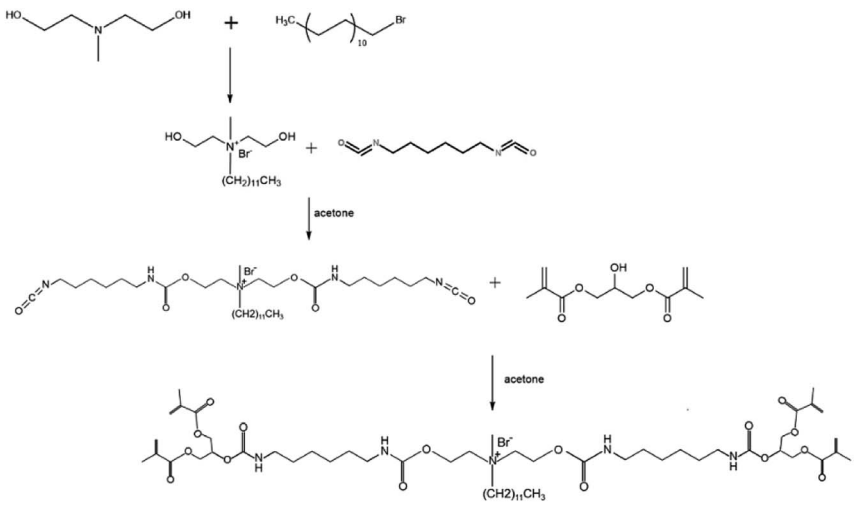

Fig. 1 Synthesis route of TMQA.

Table 2 MIC and MBC values (μg mL^{-1}) of three materials determined for *Streptococcus mutans*

	MIC	MBC
TMQA	7.81	31.3
MAE-DB	7.81	15.6
Chlorhexidine acetate	3.91	7.81

ability is still in the same order of magnitude as these strong antimicrobials.

Representative SEM images of the adherence of *Streptococcus mutans* biofilms on the polymerized resin disks after 24 h of anaerobic culturing are collectively shown in Fig. 2. Thick biofilms with a multi-layered three-dimensional structure appear on the neat resin surface. As the concentration of TMQA increases, the bacteria deform, shrunk, fuse, lyse and produce cell debris.

The TM7 and TM10 groups were almost entirely cell debris, leaving only a small amount of survive bacteria that were not in contact with the resin.

Representative CLSM images of biofilms with a Live/Dead stain are shown in Fig. 3. As the TMQA concentration increased, the number of viable bacteria decreased, whereas the number of dead bacteria increased, and almost no viable bacteria were present on the surfaces of the TM7 and TM10 groups.

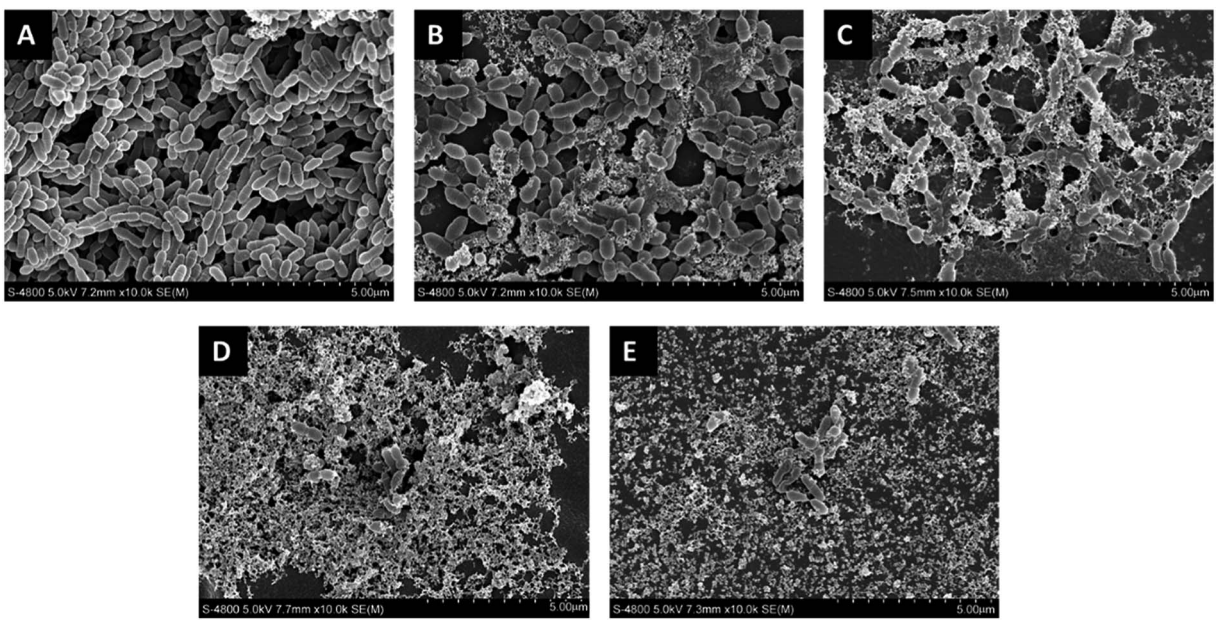

Fig. 2 Representative SEM images of *Streptococcus mutans* biofilms on experimental resin surfaces after 24 h of aerobic growth in BHI medium: (A) TM0, (B) TM1, (C) TM4, (D) TM7, (E) TM10.

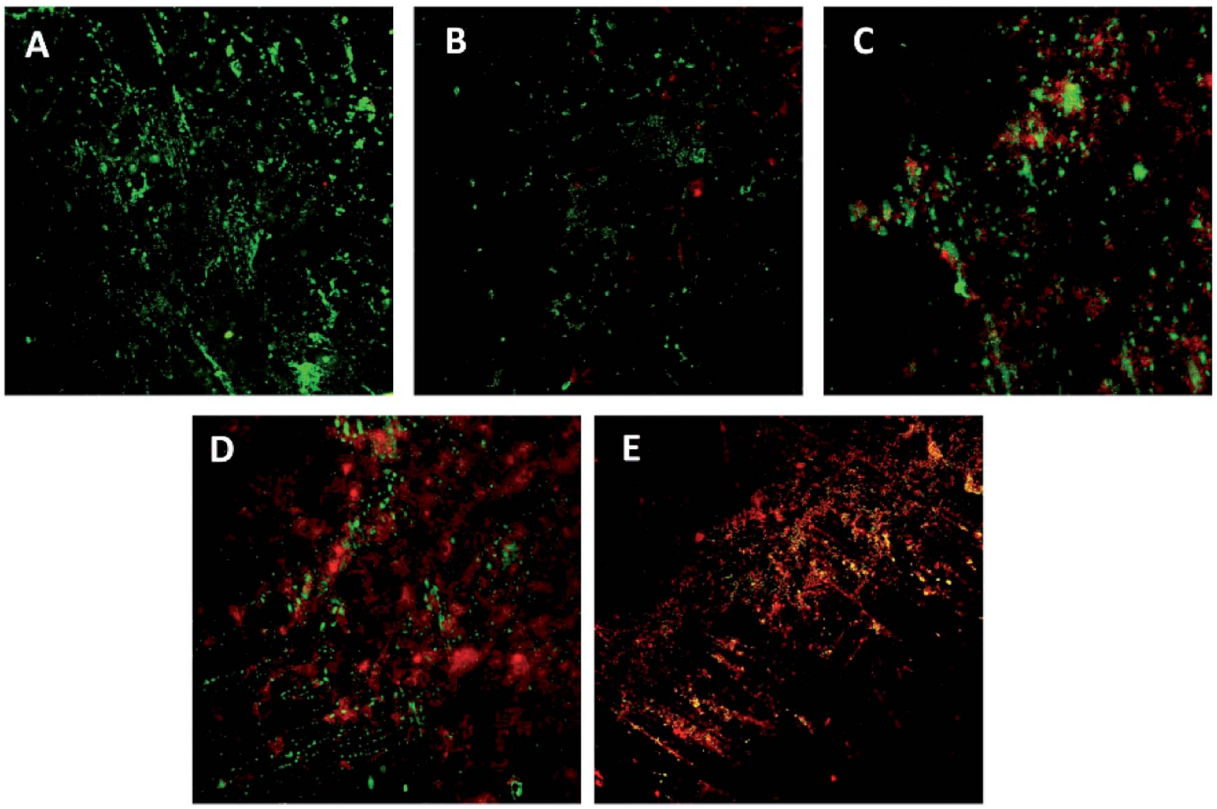

Fig. 3 Representative CLSM images of Live/Dead-stained biofilms after 24 h of anaerobic growth on the tested material surfaces: (A) TM0, (B) TM1, (C) TM4, (D) TM7, (E) TM10. Live bacteria exhibited green fluorescence, and bacteria with compromised membranes exhibited red fluorescence.

3.4 Degree of conversion

The values of the degree of conversion are listed in Table 3. As the TMQA content increases, the DC of the resin continues to decrease. Statistical analyses show there are no significant differences between the TM0, TM1, and TM4 groups. The DC of the TM7 and TM10 groups was significantly lower than that of the TM0 group ($P < 0.05$).

3.5 Contact angle

The values of the contact angle are shown in Table 3 and Fig. 5. The differences in the contact angles of all materials are small. There is no statistical difference in the contact angles of all materials.

3.6 Water sorption, solubility, and diffusion coefficient

The values of the WS and SL are shown in Table 3 and Fig. 5. The WS and SL first decrease and then increase as the proportion of TMQA increases. Resins containing low concentrations of TMQA (TM1 and TM4) had a lower WS and SL than the control group. The WS and SL of TM4 group were significantly lower than those of DB4 group ($P < 0.05$). The SL of DB4 group was higher than control group ($P < 0.05$). Resins containing high concentrations (TM7 and TM10) had a significantly higher WS and SL than the control group ($P < 0.05$). The TM4 group had the lowest WS and SL, while the TM10 group had the highest WS and SL.

Table 3 Degree of conversion (DC), contact angle, water sorption (WS), solubility (SL), and diffusion coefficient (D) of experimental dental resin composites[a]

	DC (%)	Contact angle (°)	WS (μg mm^{-3})	SL (μg mm^{-3})	D (10^{-8} cm^2 s^{-1})
TM0	62.22 ± 1.98^{A}	61.6 ± 3.3^{A}	33.26 ± 3.12^{A}	8.51 ± 0.39^{A}	0.92 ± 0.075^{AC}
TM1	61.32 ± 2.14^{A}	59.2 ± 3.2^{A}	29.3 ± 5.6^{A}	7.02 ± 0.28^{B}	0.82 ± 0.071^{AB}
TM4	59.6 ± 2.15^{AB}	60.4 ± 4.3^{A}	26.91 ± 3.99^{A}	6.72 ± 0.3^{B}	0.68 ± 0.043^{B}
TM7	56.1 ± 1.17^{BC}	64.6 ± 4.2^{A}	42.79 ± 3.56^{B}	9.82 ± 0.29^{C}	1.07 ± 0.11^{C}
TM10	54.58 ± 1.64^{CD}	63.3 ± 4.9^{A}	46.6 ± 2.32^{B}	11.52 ± 0.4^{D}	1.26 ± 0.12^{D}

[a] Different uppercase letters represent statistically significant differences in same column ($P < 0.05$).

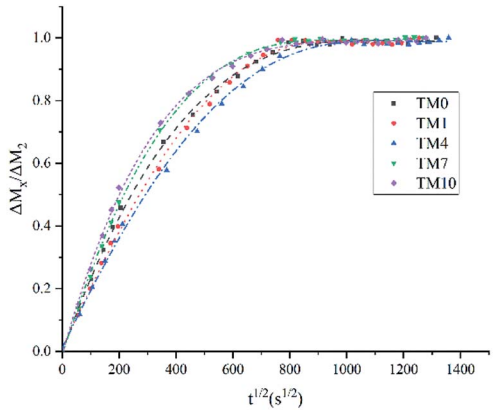

Fig. 4 Rate of water sorption for resin prepared from different concentrations of TMQA (mean values of five replicates).

Plots of $\Delta M_t/\Delta M_2$ against $t^{1/2}$ are given for resins containing different concentrations of TMQA in Fig. 4, which shows that $\Delta M_t/\Delta M_2$ *vs.* $t^{1/2}$ exhibits a straight line in the earlier stages. Then, M_t gradually reaches mass M_2 at equilibrium within about 7 days ($t^{1/2} \approx 800$). The diffusion coefficients of water (D) were calculated using Stefan's approximation when $\Delta M_t/\Delta M_2 \leq 0.5$, as shown in Table 3. The D value of the TM1 group was comparable to that of the TM0 group ($P > 0.05$). The TM4 group had a lower D than the TM0 group ($P < 0.05$), while the TM7 and TM10 groups had higher D values than the TM0 group ($P < 0.05$).

3.7 DMA

The values of the polymer network heterogeneity and crosslink density (υ) are presented in Fig. 6B. Both the heterogeneity value and crosslink density value increase first and decrease afterward with an increase in the concentrations of TMQA. The TM4 group showed the highest heterogeneity value and crosslink density value of all the dental resins.

3.8 Cytotoxicity and viability experiments

The cell proliferation activity of L929 cells after exposure to different resin extracts for 1, 3, and 5 days are shown in Fig. 7. After 1 day of culture in the different resin extracts, the number of cells in the negative control (NC) group was the highest, while the number of cells in the SB group was the lowest. The numbers of cells in all of the experimental groups (TM0, TM1, TM4, TM7, and TM10) were lower than that in the NC group. With an increase in the number of culture days, the number of cells in all TMQA groups increased exponentially, presenting a typical polygonal shape. There were no significant differences

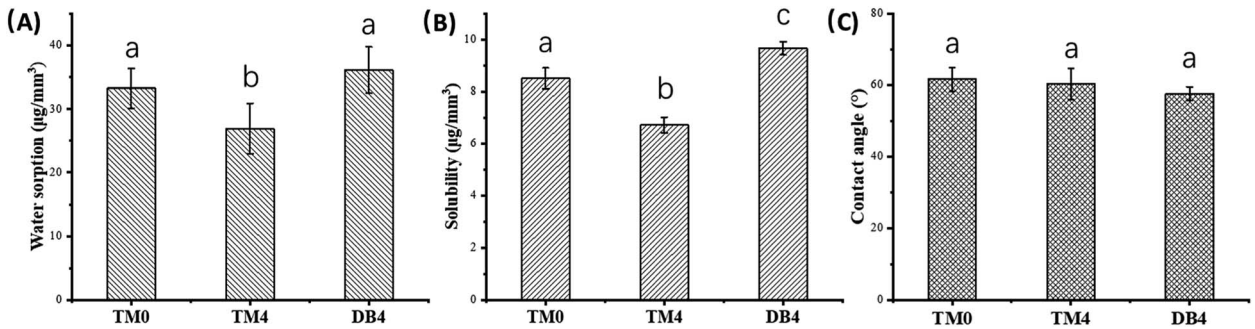

Fig. 5 Physical properties of resins with 0% TMQA, 4% TMQA and 4% MAE-DB ((A) water sorption; (B) solubility; (C) contact angle). Different lowercase letters represent statistically significant differences in same picture ($P < 0.05$).

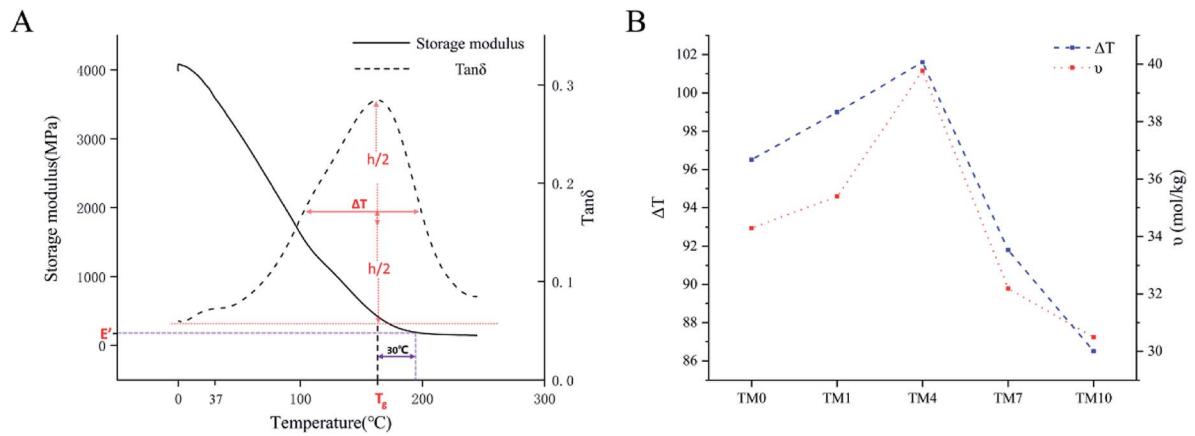

Fig. 6 (A) Typical storage modulus and tan δ curve to T_g, E, E' and ΔT. (B) ΔT and υ of resins with different concentrations of TMQA.

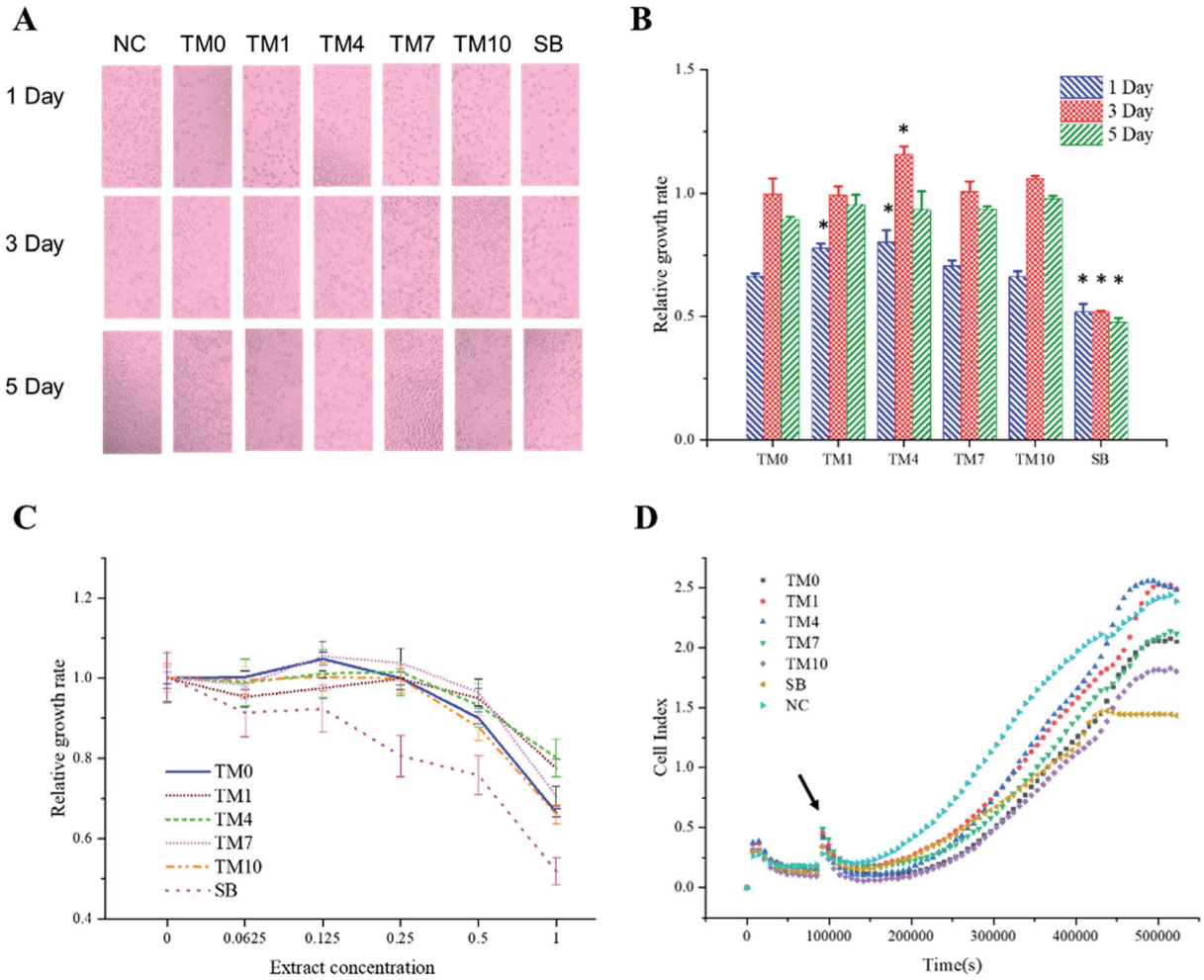

Fig. 7 Cell proliferation activity after 1, 3, and 5 days of culture in different resin extracts. (A) L929 cell morphology and number after 1, 3, and 5 days of culture. (B) Relative growth rate of L929 cells after 1, 3, and 5 days of culture. Asterisk indicates statistical difference from TM0 group. (C) Relative growth rate of L929 cells after 1 day of culture at different concentrations of resin extracts. (D) Real-time monitoring of L929 cells infected with different resin extracts using RTCA system. At indicated time point, cells were inoculated with serial resin extracts.

in the cell morphology and number for all groups except the SB group after 3 and 5 days of culture.

The number of cells in the SB group was the lowest, with the number of typical polygonal cells decreasing and some cell fragments seen after 5 days of culture. Fig. 7B also shows that the relative cell growth rate of the SB group is minimal after 1, 3, and 5 days of culture. The relative cell growth rate of the SB group is statistically different from that of TM0. With an increase in the TMQA concentrations in the resins, the cell proliferation activity increased first and then decreased, and the highest activity was found in the TM4 group. There was no significant difference in the relative growth rate of cells between the TM10 and TM0 groups after 1, 3, and 5 days of culture.

Fig. 7C shows the relative growth rate of each group for different concentrations of resin extracts after 1 day of cell culture. For all experimental groups with different grade concentrations, there were no significant changes in the relative growth rate when the concentration was lower than 0.25. When the concentration was higher than 0.25, the cell proliferation activity decreased with an increase in the concentrations. When the concentration of the SB2 group was lower than 0.125, the cell proliferation activity did not change significantly. When the concentration was higher than 0.125, the cell proliferation activity decreased with an increase in the concentrations.

Fig. 7D shows that as the culture time increased, the number of cells rose slowly owing to cell proliferation. All of the experimental groups (TM0–10) had lower cell indices than the NC group after 5 days of culture. The TM1 and TM4 groups had higher cell indices than the TM0 group. The SB group reached a plateau first owing to cellular confluence, and had the lowest cell index.

4. Discussion

There is no chemical bond between branched polymers, and in theory they are still similar in structure to linear polymers. However, when a chemical bond is formed between the side chains of the same or different macromolecules, the polymer

forms a network-like structure. The size of the network depends on the number of chemical bonds that are crosslinked between the polymer branches. After crosslinking of the polymer, the rotation and movement of the molecule are greatly restricted. Thus, the macroscopic strength and rigidity of the polymer can be increased. In the laboratory, we need resins with higher strength and stiffness, so we need to increase the crosslink density of the resins. Most of the previous quaternary ammonium salt monomers contained only one or two reactive methacrylate groups. The monomers were often dangling in the polymer network, and the degree of crosslinking was low. TMQA can become a crosslinking center in a polymer network because it has four reactive methacrylate groups. The DMA results show that the heterogeneity and crosslinking degree of the resins increase first and then decrease after the addition of TMQA. Resins incorporating too-high concentrations of TMQA beyond the polymerizable capability of the resin polymer network may adversely affect the structural properties of the resins. This is mainly owing to the fact that the molecular weight of the TMQA is relatively high, and the viscosity of the resin matrix system increases after the addition of a large amount. Thus, the mobility of the monomer during the polymerization process is affected.

SEM results showed that TMQA-modified resin had significant antibacterial properties, and that the antibacterial effect increased with the increase in the QAS monomer concentration. When the concentration of both types of QAS was more than 4%, the bacteria could not form complete biofilms on the resin surface, and numerous lysed or shrunken bacteria and bacterial debris appeared. CLSM also showed similar results, and with an increase in the TMQA concentration, the antimicrobial properties of the modified resin continuously increased, the number of viable bacteria decreased, and the number of dead bacteria increased. The antibacterial properties of QAS monomers are based on the cationic immobilization mechanism.[45] They mainly rely on positively charged quaternary ammonium groups to attract negatively charged bacteria. After contact with bacteria long-chain alkyl groups in quaternary ammonium salt monomers can penetrate the cell wall and react with the phospholipid bilayer in the cell membrane, destroying the cell membrane structure, leading to cytoplasmic exposure and causing bacterial death.[10] Thus, TMQA are dependent on kill-on-contact microbiocidal activities that can limit the biofilm maturation by reducing the bacterial adhesion and killing adventitious bacteria.

It was reported that the water sorption of the copolymer was influenced by the hydrophobicity[46] and crosslinking density of resins.[47] An increased hydrophobicity and crosslinking density of resins can reduce the water sorption of the copolymers.[48] In this work, the relative hydrophilicity of the copolymers was investigated by comparing the contact angles, which were measured using water droplets on the surface of the polymerized resins. The result showed that there is no statistical difference in the contact angles ($P > 0.05$). This indicates that the addition of TMQA has no effect on the hydrophilicity of the resins because different parts of the QAS monomer have opposite effects on the hydrophilicity and hydrophobicity of the material. The presence of both positive and negative charges in the structure of quaternary ammonium salt lead to increased hydrophilicity in the resin material.[49] The surface reorientation of the long alkyl chains of the quaternary ammonium functionalities after polymerization lead to an increased hydrophobicity of the resin material.[50] TMQA has no effect on the hydrophilicity of the resin, which may be the result of the offset between the two opposite effects. Therefore, the water absorption of the resin is less related to the hydrophilicity of TMQA, which is mainly affected by the crosslink density of the resins. The trend of water absorption in this study is consistent with the results of the crosslinking density in DMA, which increases first and then decreases with an increase in TMQA.

The water solubility of the copolymers is related to the amount of unreacted monomers in the crosslinking networks, and to the characteristics of the networks and monomers.[47] The results show that the addition of a high concentration of TMQA in resin groups (TM7 and TM10) can increase the water solubility of the resins. This is because a large proportion of TMQA resulted in a decrease in DC and an increase in unreacted monomers. The addition of a low concentration of TMQA (TM1 and TM4) can reduce the water solubility of the resins even though they have a DC similar to that of the control group. If a tetrafunctional methacrylate molecule binds to the polymer network, at least one of the four methacrylate groups can react. However, for bis-GMA and TEGDMA molecules to be combined, at least one of the two methacrylate groups should react. That is, when the DC is similar, the unreacted monomer content of resins with four methacrylate groups must be lower than that of resins with two methacrylate groups.[51]

Therefore, although the experimental groups containing small concentrations of TMQA have similar DCs to the control group, the number of unreacted monomers in the groups with a small concentration of TMQA was lower than that of the control group. On the other hand, the bulky structure of TMQA made it difficult to leach out of the crosslinking network. The diffusion coefficient reflects the ability of water molecules to migrate in the polymer and the structural properties of the polymer product. It is determined by the crosslink density of the polymer and the mobility of the polymer segment. A polymer network structure with a high crosslink density and low mobility has a small diffusion coefficient.[40] The diffusion coefficient of TM4 is the smallest, indicating that it has the highest crosslink density and the smallest mobility of the polymer chains. A decrease in the water solubility and diffusion coefficient results in increased biocompatibility, which is consistent with the cytotoxicity test of this study.

The cytotoxicity of dental resin materials is mostly caused by the infiltration of free monomers with incomplete polymerization. Therefore, a cytotoxicity test of the extracts after polymerization of the experimental materials was carried out in this study. The results showed that the cell proliferation activity of the SB group was the lowest, and with an increase in TMQA concentrations, the cell proliferation activity increased first and then decreased. The main reason for the increase in cell proliferation activity after adding a small amount of TMQA is that the addition of TMQA can increase the degree of

crosslinking of the resin, resulting in a decrease in the number of unpolymerized monomers in the resin and fewer unpolymerized monomers in the leachate.

When the TMQA content exceeds 4%, the cell proliferation activity decreases, mainly because some of the TMQA may also leach into the extracts. TMQA, as a quaternary ammonium salt monomer, is similar to HEMA and other traditional dental monomers. It can destroy the redox balance of cells.[10,52] Single bond 2 is one of the commonly used adhesives in clinics. There are few symptoms such as post-operative sensitivity and pain in the clinic, and its biological safety is acceptable. However, in our study, the SB group showed minimal cell proliferation activity, probably because parts of the hydrophilic monomer HEMA and organic solvent were added to reduce viscosity and increase permeability. Geurtsen[53] believes that hydrophilic HEMA monomers are more likely to precipitate out on the first day after polymerization than other unpolymerized monomers, and even free monomers can precipitate into saliva during the initial stages of polymerization.

Although HEMA is less cytotoxic, direct infiltration into the extract will result in a decrease in bacterial proliferative activity. The relative growth rate of cells is the ratio between the mean absorbance value of the experimental groups and the mean absorbance value of the control. Therefore, the relative growth rate is close to 1, which indicates that the cell growth rate of the experimental groups is similar to that of the blank control group, and the cytotoxicity of the experimental group material is low. Fig. 7B shows that the relative growth rate of all experimental groups was the lowest on the first day and increased to 1 on the second and third days. This indicates that the cell proliferation of the experimental group on the second and third days was similar to that of the blank control group. Fig. 7A also shows that there was no significant change in the number and morphology of cells in all experimental groups relative to the negative control group. Therefore, the effect of the experimental material on cell proliferation is transient.

The relative growth rate of the cells in the SB group was much lower than 1 after 1, 3, and 5 days of culture, and the morphology of the cultured cells changed significantly after 5 days. The cell proliferation activity of all experimental groups was higher than that of the SB group, and its cell proliferation activity gradually recovered when the culture time was prolonged. In addition, there was no significant difference in the relative growth rate of cells between the TM10 and TM0 groups after 1, 3, and 5 days of culture, indicating that the largest amount of added TMQA did not increase the cytotoxicity of the resin in this study. The above evidence proves that the biosafety of TMQA is completely acceptable.

5. Conclusions

A tetrafunctional methacrylate-based polymerizable quaternary ammonium monomer TMQA was synthesized and used to prepare antibacterial dental resins with high crosslink density and good biosafety. The study showed that resins with a certain amount of TMQA can reduce the water absorption and solubility and increase the heterogeneity and crosslink density compared to TMQA-free resins. Based on the outstanding comprehensive physicochemical properties of resins containing TMQA, TMQA has the potential to be used in commercial dental resins as an antibacterial monomer.

Conflicts of interest

The authors state no conflict of interest.

Acknowledgements

This work was supported financially by the National Natural Science Foundation of China (81600916, 81701030).

References

1 R. A. Bagramian, F. Garcia-Godoy and A. R. Volpe, *Am. J. Dent.*, 2009, **22**, 3–8.
2 P. Totiam, C. González-Cabezas, M. R. Fontana and D. T. Zero, *Caries Res.*, 2007, **41**, 467–473.
3 L. Tjäderhane, M. A. R. Buzalaf, M. Carrilho and C. Chaussain, *Caries Res.*, 2015, **49**, 193–208.
4 Z. Khurshid, M. Zafar, S. Qasim, S. Shahab, M. Naseem and A. AbuReqaiba, *Materials*, 2015, **8**, 717–731.
5 N. Alvanforoush, J. Palamara, R. H. Wong and M. F. Burrow, *Aust. Dent. J.*, 2017, **62**, 132–145.
6 L. Xiaoxu, Q. Huang, F. Liu, J. He and Z. Lin, *J. Appl. Polym. Sci.*, 2013, **129**, 3373–3381.
7 X. Xu, Y. Wang, S. Liao, Z. T. Wen and Y. Fan, *J. Biomed. Mater. Res., Part B*, 2014, **100**, 1151–1162.
8 S. Tantanuch, B. Kukiattrakoon, T. Peerasukprasert, N. Chanmanee, P. Chaisomboonphun and A. Rodklai, *J. Conservative Dent.*, 2016, **19**, 51–55.
9 L. Cheng, K. Zhang, N. Zhang, M. a. S. Melo, M. D. Weir, X. D. Zhou, Y. X. Bai, M. A. Reynolds and H. H. K. Xu, *J. Dent. Res.*, 2017, **96**, 855–863.
10 Y. Jiao, L. Niu, S. Ma, J. Li, F. R. Tay and J. Chen, *Prog. Polym. Sci.*, 2017, **71**, 53–90.
11 G. do Amaral, T. Negrini, M. Maltz and R. Arthur, *Aust. Dent. J.*, 2016, **61**, 6–15.
12 A. M. Young, in *Drug-Device Combination Products*, Elsevier, 2010, pp. 246–279.
13 R. S. Tobias, *Int. Endod. J.*, 2007, **21**, 155–160.
14 L. Chen, H. Shen and B. I. Suh, *Am. J. Dent.*, 2012, **25**, 337–346.
15 N. Beyth, S. Farah, A. J. Domb and E. I. Weiss, *React. Funct. Polym.*, 2014, **75**, 81–88.
16 N. Zhang, K. Zhang, X. Xie, Z. Dai, Z. Zhao, S. Imazato, Y. A. Al-Dulaijan, F. D. Al-Qarni, M. D. Weir, M. A. Reynolds, Y. Bai, L. Wang and H. H. K. Xu, *Nanomaterials*, 2018, **8**, 393.
17 S. Imazato and J. F. McCabe, *J. Dent. Res.*, 1994, **73**, 1641–1645.
18 Y. Ge, S. Wang, X. Zhou, H. Wang, H. H. K. Xu and L. Cheng, *Materials*, 2015, **8**, 3532–3549.
19 H. Murata, R. R. Koepsel, K. Matyjaszewski and A. J. Russell, *Biomaterials*, 2007, **28**, 4870–4879.

20 F. Li, M. D. Weir, J. Chen and H. H. K. Xu, *Dent. Mater.*, 2014, **30**, 433–441.
21 C. J. Ioannou, G. W. Hanlon and S. P. Denyer, *Antimicrob. Agents Chemother.*, 2007, **51**, 296–306.
22 R. Müller, A. Eidt, K.-A. Hiller, V. Katzur, M. Subat, H. Schweikl, S. Imazato, S. Ruhl and G. Schmalz, *Biomaterials*, 2009, **30**, 4921–4929.
23 S. Imazato, R. R. B. Russell and J. F. McCabe, *J. Dent.*, 1995, **23**, 177–181.
24 S. Imazato, *Biomaterials*, 1999, **20**, 899–903.
25 Y.-H. Xiao, S. Ma, J.-H. Chen, Z.-G. Chai, F. Li and Y.-J. Wang, *J. Biomed. Mater. Res., Part B*, 2009, **90**, 813–817.
26 L. Huang, F. Yu, X. Sun, Y. Dong, P. Lin, H. Yu, Y. Xiao, Z. Chai, X. Xing and J. Chen, *Sci. Rep.*, 2016, **6**, 3858.
27 Y. Liu, L. Zhang, L. Niu, T. Yu, H. H. K. Xu, M. D. Weir, T. W. Oates, F. R. Tay and J. Chen, *J. Dent.*, 2018, **72**, 53–63.
28 L. Cheng, M. D. Weir, H. H. K. Xu, J. M. Antonucci, A. M. Kraigsley, N. J. Lin, S. Lin-Gibson and X. Zhou, *Dent. Mater.*, 2012, **28**, 561–572.
29 X. Feng, N. Zhang, H. H. K. Xu, M. D. Weir, M. A. S. Melo, Y. Bai and K. Zhang, *Dent. Mater. J.*, 2017, **36**, 669–676.
30 Y. W. Yang, F. Yu, H. C. Zhang, Y. Dong, Y. N. Qiu, Y. Jiao, X. D. Xing, M. Tian, L. Huang and J. H. Chen, *Int. Endod. J.*, 2017, **51**, 26–40.
31 F. Li, M. D. Weir, A. F. Fouad and H. H. K. Xu, *J. Dent.*, 2013, **41**, 881–891.
32 L. Huang, Y. Xiao, X. Xing, F. Li, S. Ma, L. Qi and J. Chen, *Arch. Oral Biol.*, 2011, **56**, 367–373.
33 M. Jaymand, M. Lotfi, J. Barar and S. Kimyai, *Res. Chem. Intermed.*, 2017, **43**, 5707–5722.
34 M. Jaymand, M. lotfi and M. Abbasian, *Mater. Res. Express*, 2018, **5**, 035406.
35 M. Jaymand, M. Lotfi and R. Lotfi, *RSC Adv.*, 2016, **6**, 43127–43146.
36 L. G. Schultz, Y. Zhao and S. C. Zimmerman, *Angew. Chem., Int. Ed. Engl.*, 2001, **40**, 1962–1966.
37 L. Huang, F. Yu, X. Sun, Y. Dong, P. Lin, H. Yu, Y. Xiao, Z. Chai, X. Xing and J. Chen, *Sci. Rep.*, 2016, **6**, 33858.
38 Y. Yang, L. Huang, Y. Dong, H. Zhang, W. Zhou, J. Ban, J. Wei, Y. Liu, J. Gao and J. Chen, *PLoS One*, 2014, **9**, e112549.
39 I. Sideridou, D. S. Achilias, C. Spyroudi and M. Karabela, *Biomaterials*, 2004, **25**, 367–376.
40 J. Malacarne, R. M. Carvalho, M. F. de Goes, N. Svizero, D. H. Pashley, F. R. Tay, C. K. Yiu and M. R. de O. Carrilho, *Dent. Mater.*, 2006, **22**, 973–980.
41 L. C. Yamasaki, A. G. De Vito Moraes, M. Barros, S. Lewis, C. Francci, J. W. Stansbury and C. S. Pfeifer, *Dent. Mater.*, 2013, **29**, e169–e179.
42 S. Luo, F. Liu and J. He, *J. Mech. Behav. Biomed. Mater.*, 2019, **94**, 222–228.
43 Y. W. Yang, F. Yu, H. C. Zhang, Y. Dong, Y. N. Qiu, Y. Jiao, X. D. Xing, M. Tian, L. Huang and J. H. Chen, *Int. Endod. J.*, 2018, **51**, 26–40.
44 H. Benachour, T. Bastogne, M. Toussaint, Y. Chemli, A. Sève, C. Frochot, F. Lux, O. Tillement, R. Vanderesse and M. Barberi-Heyob, *PLoS One*, 2012, **7**, e48617.
45 S. Liu, L. Tonggu, L. Niu, S. Gong, B. Fan, L. Wang, J. Zhao, C. Huang, D. H. Pashley and F. R. Tay, *Sci. Rep.*, 2016, **6**, 21882.
46 G. Sokolowski, A. Szczesio, K. Bociong, K. Kaluzinska, B. Lapinska, J. Sokolowski, M. Domarecka and M. Lukomska-Szymanska, *Materials*, 2018, **11**, 973.
47 J. He, F. Liu, Y. Luo and D. Jia, *J. Appl. Polym. Sci.*, 2012, **125**, 114–120.
48 J. He, F. Liu, Y. Luo and D. Jia, *J. Appl. Polym. Sci.*, 2012, **126**, 1527–1531.
49 P. Makvandi, M. Ghaemy and M. Mohseni, *Eur. Polym. J.*, 2016, **74**, 81–90.
50 S. Gong, L. Niu, L. K. Kemp, C. K. Y. Yiu, H. Ryou, Y. Qi, J. D. Blizzard, S. Nikonov, M. G. Brackett, R. L. W. Messer, C. D. Wu, J. Mao, L. Bryan Brister, F. A. Rueggeberg, D. D. Arola, D. H. Pashley and F. R. Tay, *Acta Biomater.*, 2012, **8**, 3270–3282.
51 C.-M. Chung, M.-S. Kim, J.-G. Kim and D.-O. Jang, *J. Biomed. Mater. Res.*, 2002, **62**, 622–627.
52 M. Sai, S. Le-qun, X. Yu-hong, L. Fang, H. Li, L. Shen and C. Ji-hua, *Braz. J. Med. Biol. Res.*, 2011, **44**, 1125–1133.
53 W. Geurtsen, *Crit. Rev. Oral Biol. Med.*, 2000, **11**, 333–355.